NUMERICAL SIMULATIONS OF FAST MHD WAVES IN A CORONAL PLASMA

IV. *Impulsively Generated Nonlinear Waves*

K. MURAWSKI and B. ROBERTS

Department of Mathematical and Computational Sciences, University of St. Andrews, Fife KY16 9SS, Scotland

(Received 10 April, 1992; in revised form 17 July, 1992)

Abstract. The temporal evolution of ducted waves in coronal loops (represented by smoothed slabs of enhanced gas density embedded within a uniform magnetic field) is studied in the framework of cold magnetohydrodynamics by means of numerical simulations. The numerical results show that there is an energy leakage from the slab, associated with the propagation of wave packets which exhibit periodic, quasi-periodic and decay phases. Even for weak slabs the nonlinearity can play a significant role, leading to wave breaking and shifted time signatures in comparison to the corresponding signatures of linear waves. The quasi-periodic phase possesses the strongest amplitudes in an event, making this phase the most significant for observations.

1. Introduction

Impulsively generated coronal linear pulsations were first discussed from a theoretical standpoint by Roberts, Edwin, and Benz (1983, 1984). Subsequently, Ren-Yang *et al.* (1990) and Qi-Jun *et al.* (1990) have provided examples of events with characteristic second-order time scales which possess many of the features predicted by the theory in Roberts, Edwin, and Benz (1984). Pulsations and oscillations observed by Tapping (1978), Harrison (1987), and Pasachoff (1990) would also seem to admit of interpretations in terms of magnetohydrodynamic waves (see the review by Edwin, 1992). Added to this is the long history of short period (1 s) pulsations detected in radio events (Krüger, 1979; Aschwanden, 1987) and there are similar short period oscillations reported in microwaves and hard X-rays (Takakura *et al.*, 1983; Kane *et al.*, 1983).

The theory developed in Roberts, Edwin, and Benz (1984) shows that when a linear disturbance is impulsively excited within a high gas density, low Alfvén speed region, such as provided by a coronal loop, then fast MHD waves are guided by the structure and exhibit three phases. At a given observation location far from the impulsive source, the passage of a fast MHD wave results in first the occurrence of a small amplitude regular oscillations (the periodic phase of the event). Then, after a while, the periodic phase gives way to larger amplitude, more rapid pulsations (the quasi-periodic phase). Finally, the quasi-periodic gives way to a decay phase as the wave packet created by the impulsive source passes beyond the observation location. The time scales and durations of these phases are predicted by the linear theory of Roberts, Edwin, and Benz (see also Murawski and Roberts, 1993b, Paper II) and thus they are valid for small amplitude perturbations.

Solar Physics **145:** 65–75, 1993.

In this paper we consider numerically the case of a smoothed density profile. We investigate the time scales of a ducted fast magnetosonic waves in a low-β plasma, and determine how leakage from the duct takes place as the nonlinear wave adjusts to its natural configuration. We explore how the time scales depend on amplitude and the initial location of the disturbance.

2. Mathematical Model

A coronal loop is modelled by a cold slab of plasma with gas density profile $\rho = \rho_0(x)$ that extends indifinitely in the $y - z$ plane, has width $2a$ in the x-direction and has the z-axis as its central axis. The slab is almost uniform throughout the x-direction except for a narrow transition region representing the smeared boundary of the slab. See Murawski and Roberts (1993a, Paper I). The slab density is ρ_0 in the centre and ρ_e in the far environment. Specifically, we take

$$\rho_0(x) = \begin{cases} \rho_0\,, & |x| \leq a\,, \\ \rho_e + (\rho_0/\rho_e - 1)\rho_e/\cosh^{14}(x - a)\,, & x > a\,. \end{cases} \tag{2.1}$$

A uniform magnetic field $\mathbf{B}_0$ lies in the z-direction.

Consider nonlinear oscillations of density ρ, vector magnetic potential $\mathbf{A} = [0, A, 0]$, with $\mathbf{B} = \nabla \times \mathbf{A}$, and velocity $\mathbf{V} = [u, 0, w]$. Normalizing ρ by ρ_0, $\mathbf{V}$ by V_A (the internal Alfvén speed), x and z by a, A by $B_0 a$, the cold plasma equations can be written

$$\rho_t + (\rho u)_x + (\rho w)_z = 0\,, \tag{2.2}$$

$$u_t + uu_x + wu_z = -\rho^{-1}(A_{xx} + A_{zz})A_x\,, \tag{2.3}$$

$$w_t + uw_x + ww_z = -\rho^{-1}(A_{xx} + A_{zz})A_z\,, \tag{2.4}$$

$$A_t = -(wA_z + uA_x)\,. \tag{2.5}$$

These equations form the subject of our numerical analysis presented in the next section.

3. Numerical Method and Results

The numerical code utilizes the fast Fourier transform method in space and the modified Euler method in time:

$$g^* = g^n + \frac{\Delta t}{2} G^n\,, \tag{3.1a}$$

$$g^{n+1} = g^n + \Delta t G^*\,, \tag{3.1b}$$

where the system of Equations (2.2)–(2.5) cast in the form

$$g_t = G(g, g_x, g_z, g_{xx}, g_{zz})\,. \tag{3.2}$$

The space derivatives are computed spectrally, e.g., $g_x^n = F^{-1}imFg^n$, where F and F^{-1} denote Fourier and inverse Fourier operators, and i and m are the imaginary unit and the Fourier mode number, respectively. The nonlinear terms are integrated in a configuration space. The advantage of the fast Fourier transform method is ease of coding and high accuracy. However, a disadvantage of the method is the periodicity imposed on the solutions. A similar method was used by Murawski and Edwin (1992) to solve the Zakharov–Kuznetsov equation and Murawski and Roberts (1993a, b, c, Papers I–III) for solving MHD equations. For both the x- and z-directions, 128 Fourier modes were used with the simulation region defined by $-32 \leq x < 32$, $-32 \leq z < 32$. The temporal increment was chosen as small as possible to guarantee numerical accuracy. Standard numerical tests have been performed doubling the number of Fourier modes and halving the time step until no significant changes appeared. Additionally, numerically obtained results were checked by calculation of the integrals of motion, the mass M and the energy E:

$$M = \int_{-\infty}^{\infty} \int_{-\infty}^{\infty} \rho \, \mathrm{d}x \, \mathrm{d}z \,, \qquad E = \int_{-\infty}^{\infty} \int_{-\infty}^{\infty} [\rho(u^2 + w^2) + A_x^2 + A_z^2] \, \mathrm{d}x \, \mathrm{d}z \,. \tag{3.3}$$

Errors in the calculations were less than 2%.

An initial perturbation of the type

$$f(x, z, t = 0) = \frac{f_0}{\cosh^2(x - x_0) \cosh^2(z - z_0)} \tag{3.4}$$

was considered. (Here f represents a variable as ρ, u, w, A.) To examine numerically obtained results we also calculated the energy ratio e in the unperturbed slab (between $-1 \leq x \leq 1$ and $-32 \leq z < 32$) defined as follows:

$$e = \frac{e(t \geq 0)}{e(t = 0)} \,, \tag{3.5}$$

where

$$e(t) = \int_{-32}^{32} \left[\int_{-1}^{1} (\rho(u^2 + w^2) + A_x^2 + A_z^2) \, \mathrm{d}x \right] \mathrm{d}z \,. \tag{3.6}$$

Although $e(t)$ does not represent the total energy of the wave, because the energy of the outskirts is not included, it is closely associated with that wave energy and is convenient for computation.

Roberts, Edwin, and Benz (1984) argue that distinctive signatures, produced by a solar flare, local MHD instability or reconnection events, consist of three phases with the largest amplitudes occurring in the quasi-periodic phase (see also Paper II). This analysis has been carried out analytically for a mode of the system (Roberts, Edwin, and Benz, 1984) or numerically for a combination of modes (Paper II). Both approaches

have been made for linear waves and thus they are valid for small amplitude disturbances.

Typical gas density profiles of nonlinear waves are shown in Figure 1. The maximum of the profile grows in time for all cases we have explored and moves very slowly in time. It seems that initially humps accelerate, only to decelerate at later times. This effect is, however, very small. A plateau at the hump front and a valley at the trailing edges are noticeable at later times (see Figure 1(b)). Adjustment of the initial profile is also through pushing up very small amplitude impulses along the slab.

Whereas the gas density adjustment is on very small time scales, the time evolution of the perpendicular velocity u is quite dramatic (see Figure 2). At an early stage a valley in the middle of the hump is created (see Figure 2(b)) and some ripples start to propagate almost symmetrically outside the initial pulse location. This symmetry is progressively broken by the inhomogeneity in the Alfvén speed and in consequence trapped oscillations in the slab are apparent (see Figure 2(c)). The trapped oscillations propagate along the central axis of the slab slower than those outside the slab, and are characterized by a hump in the wavefront which is followed by a valley in the rear.

Consider the energy in the disturbance. Initially, the energy is distributed locally having two maxima at $x \simeq \pm\frac{5}{4}$, $z = 0$ and a minimum at $x = z = 0$. It then evolves in time in a similar way as in the linear case already discussed (Paper II) with some discernible ripples corresponding to outwardly propagating waves and trapped oscillations. A part of the plasma energy remains in the slab. For example, in the case of an initial disturbance with $\rho_0 = 0.1$, $u_0 = w_0 = A_0 = 0.05$ less than 0.01% of the slab energy was leaked from the slab (see Figure 3). For smaller amplitude waves (e.g., $\rho_0 = 0.1$, $u_0 = w_0 = A_0 = 0.025$), this percentage is even smaller. For larger amplitude perturbations (e.g., $\rho_0 = u_0 = w_0 = A_0 = 0.2$) the u profile is asymmetric about the plane $x = 0$ and wave breaking at $t < 5$ occurs. The transverse velocity u, calculated at the point $x = 0, z = 8$, as a function of time is presented in Figure 4. It is clear that the three phases determined by Roberts, Edwin, and Benz (1983, 1984) and Murawski and Roberts (1993b, Paper II) can be distinguished, although the periodic phase is represented by a straight horizontal line because perturbations in this phase are so small. The largest amplitude quasi-periodic phase lasts for about 8 Alfvén transit times. Assuming that in the corona the Alfvén speed $V_A = 10^3$ km s^{-1} and the loop width $2a = 1500$ km we find that this gives a duration of 6 s. Narrower loops give even smaller time scales. There is also a time scale, of 1–2 s associated with a single pulse.

It has been already stated by Roberts, Edwin, and Benz and confirmed numerically by Murawski and Roberts (1993b, Paper II) that slabs with smaller density ratio ρ_0/ρ_e lead to shorter duration times of the quasi-periodic phase. Similarly, this time can be also modified by smoother density profiles (Edwin and Roberts, 1988 and Paper II).

It is worthwhile to note that whereas the disturbed magnetic potential A evolves in time in a manner that is quite similarly to that in the perpendicular velocity u, the parallel velocity w is almost unchanged in time. However, $w(x = 0, z = 8)$ shows very small amplitude ripples arising from the initial profile as a consequence of the wave adjustment.

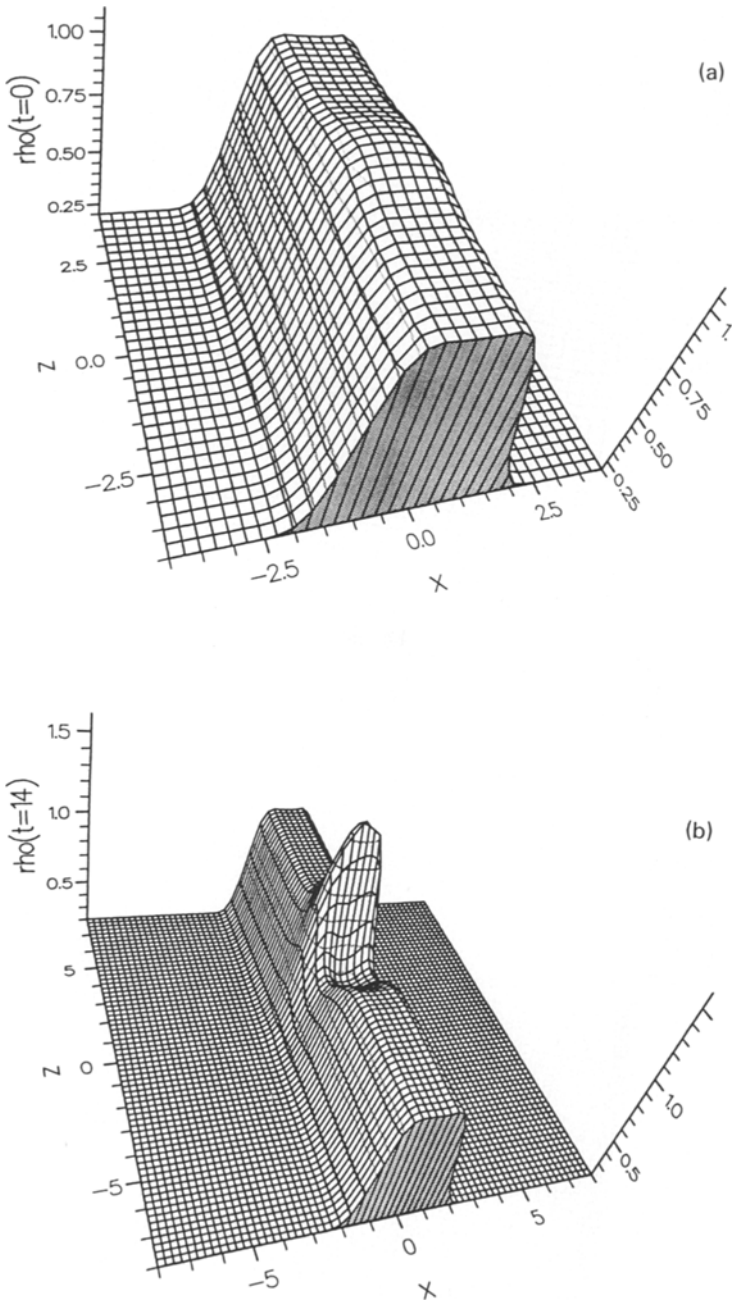

Fig. 1. Impulsively generated waves propagating in a smoothed slab (with its cross-section given by $\rho_0(x) = \rho_0$ for $|x| \leq a$ and $\rho_0(x) = \rho_e + (\rho_0/\rho_e - 1)\rho_e/\cosh^{14}(x - a)$, for $x > a$), with the gas density ratio $\rho_0/\rho_e = 5$. (a) The initial profile ($t = 0$); (b) the profile at $t = 14$. The initial profile (a) is $A(x, z, t = 0) = A_0/\cosh^2(x - x_0)/\cosh^2(z - z_0)$ with $x_0 = z_0 = 0$, $\rho_0 = 0.1$, $u_0 = w_0 = A_0 = 0.05$. Time is in units of the Alfvén transit time, a/V_A. Note the asymmetry in z of the gas density profile at $t = 14$ (case (b)).

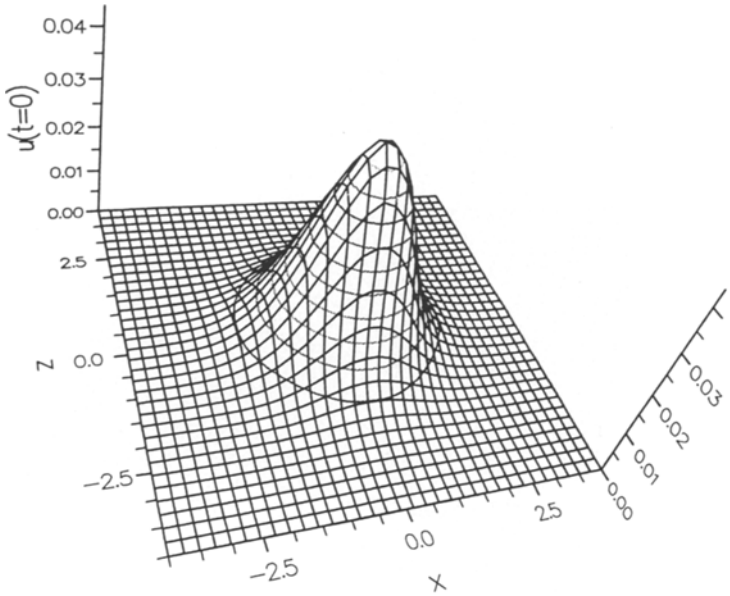
u(t=0)
0.04
0.03
0.02
0.01
0.00
2.5
Z
0.0
−2.5
−2.5
0.0
2.5
X
0.00
0.01
0.02
0.03

Fig. 2a.

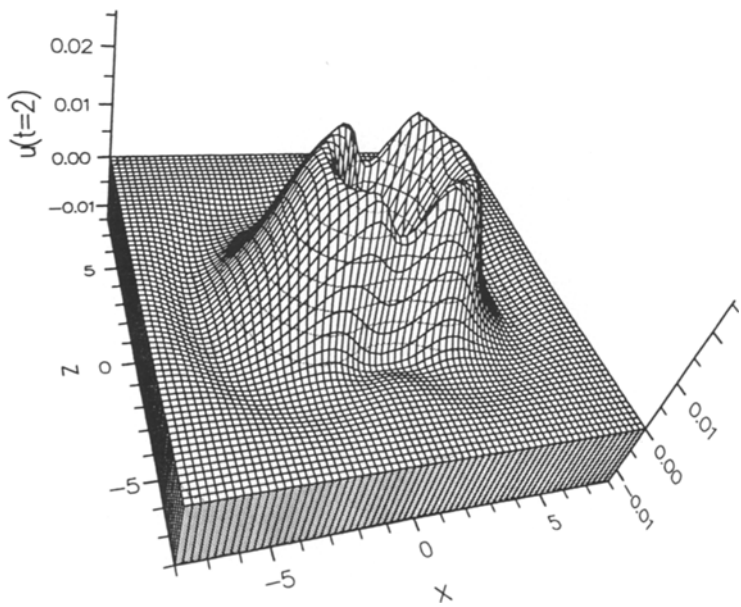
u(t=2)
0.02
0.01
0.00
−0.01
5
Z
0
−5
−5
0
5
X
0.00
0.01
−0.01

Fig. 2b.

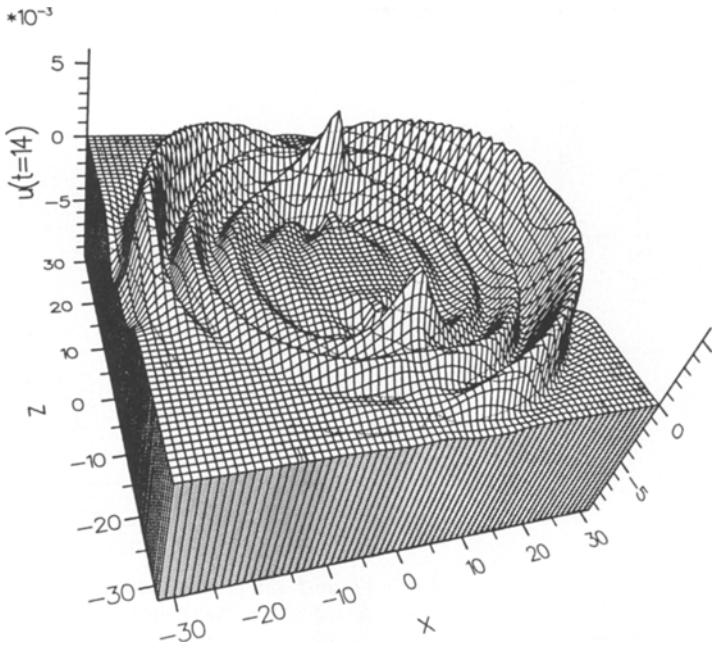

Fig. 2c.

Fig. 2. The evolution of the transverse velocity u for the pulse generated as in Figure 1. (a) The initial profile $t = 0$; (b) the profile at $t = 2$; (c) the profile at $t = 14$. The initial u profile splits into outwardly propagating waves and trapped oscillations.

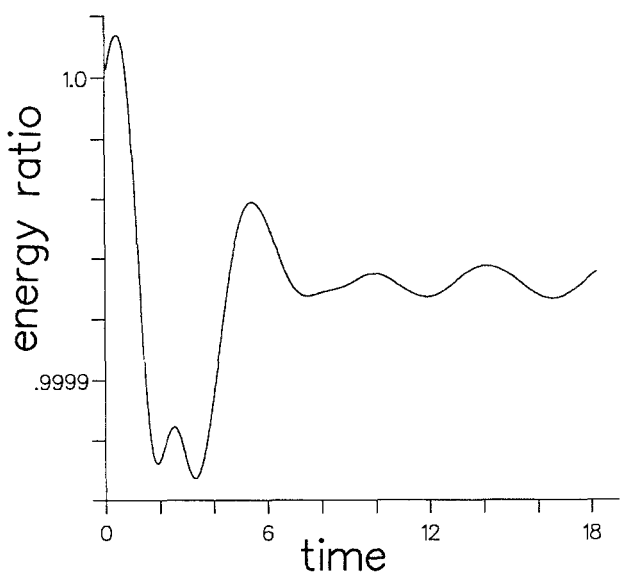

Fig. 3. The slab energy ratio as a function of time. Some of the initial energy is carried away from the slab by outwardly propagating ripples. For smaller amplitude waves there is less energy leaked from the slab.

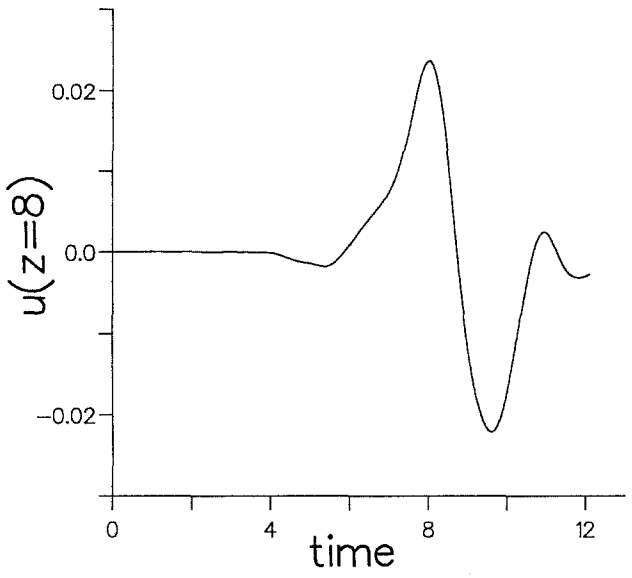

Fig. 4. The time signature of waves described in Figure 2 with pronounced quasi-periodic phase lasting from $t \simeq 4$ until $t \simeq 12$. The periodic phase is represented here by the straight horizontal line for $t < 4$. In fact, very small amplitude periodic oscillations are present for $t < 4$.

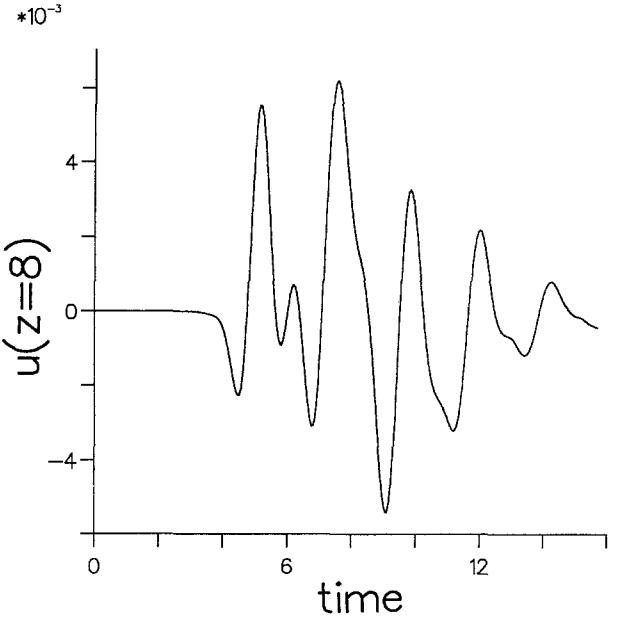

Fig. 5. The time signature of waves initially generated by a pulse located at $x_0 = 3, z_0 = 0$ and of amplitude $\rho_0 = 0.1$, $u_0 = w_0 = A_0 = 0.05$. Note the extended quasi-periodic phase.

Quite different time signatures characterize waves generated by an impulse located outside the slab. For example, the time dependence of $u(x = 0, z = 8)$ for a pulse located at $x = 3$, $z = 0$ shows an extended quasi-periodic phase with a duration time equal to about 10 Alfvén times (Figure 5), which corresponds to about 7 s. The single pulse time scale is of the order of 1 s.

Two different amplitude pulses (the smaller amplitude pulse leading the larger amplitude one), initially located at $x = , z = \pm 2$, are presented in Figure 6. They disperse in

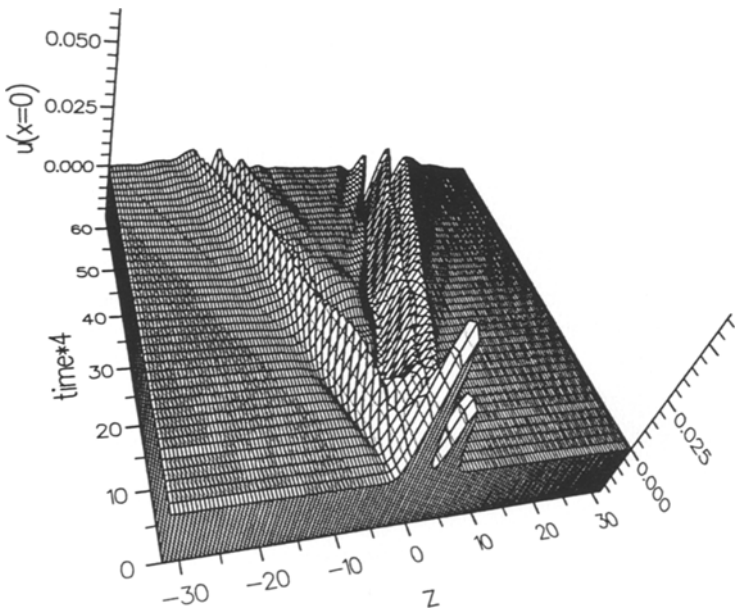

Fig. 6. The time development of trapped waves (propagating along the axis $x = 0$) such that $f(x, z, t = 0) = f_0/ch^2 x/\cosh^2(z - 2) + 2f_0/\cosh^2 x/ch^2(z + 2)$ (where f represents a variable as ρ, u, w, A), with $\rho_0 = 0.05$ and $u_0 = w_0 = A_0 = 0.025$. Initially there are two pulses with the larger one following the smaller one.

a similar way to a single pulse and undergo nonlinear interactions leading to complicated time signatures which depend on the location of the detection point. One example is presented in Figure 7 (which is made by intersecting Figure 6 by a line $z = 8$) for $u(x = 0, z = 8)$ which shows that the pulses have not yet undergone an interaction and still the smaller pulse is leading the larger one. The quasi-periodic phase lasts for about 12 Alfvén times which correspond to 9 s. It contains two maxima associated with two pulses propagating along the slab. It is interesting to note that a similar event was observed by Kurths and Karlický (1989).

In comparison to linear results, the time signatures are shifted due to nonlinearity which causes waves with larger amplitude to propagate faster. For example, in the case of $\rho_0 = 0.1$, $u_0 = w_0 = A_0 = 0.05$ the quasi-periodic phase starts at $t \simeq 5$ (see Figure 4)

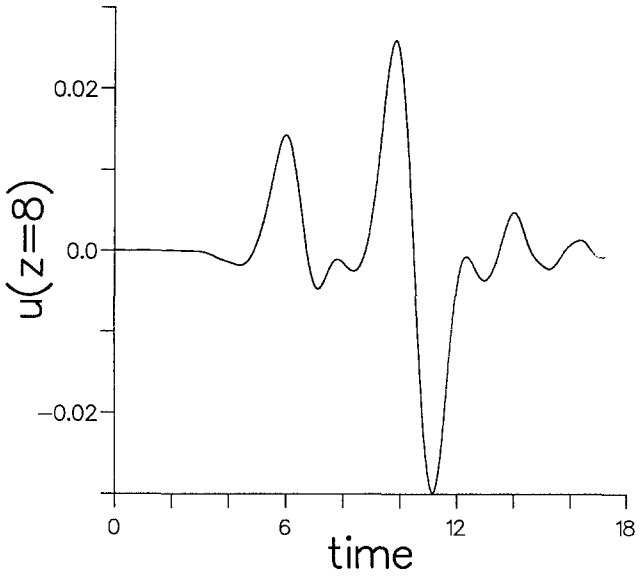

Fig. 7. The time signature of waves initially generated by the two pulses described in Figure 6. Note the complex quasi-periodic phase due to the presence of two pulses.

instead of at $t = 8$ as for the linear perturbations (Roberts, Edwin, and Benz, 1984 and Paper II).

4. Summary

Impulsively generated fast waves in a smoothed slab possess distinctive temporal signatures consisting of the three phases determined by Roberts, Edwin, and Benz (1983, 1984). Numerical simulations, presented here, give a broad agreement with the linear analysis but also provide some new features. First of all, for small amplitude waves the results are similar to those ones already obtained numerically on the basis of the linear theory (Paper II). Waves of larger amplitude propagate faster, due to the nonlinear effects, and thus all temporal signatures appear earlier than in the linear theory. Time signatures can be complex for waves either excited outside the coronal structure or in the case of a multi-series of nonlinearly interacting impulses generated at different places and times. The results prove also that large amplitude waves leak more energy from a slab than small amplitude waves.

Acknowledgements

K. M. wishes to express his sincere thanks to members of the Solar Theory Group at St. Andrews for their encouragement, help and discussion, and to the SERC for its financial support.

References

Aschwanden, M. J.: 1987, *Solar Phys.* **111**, 113.
Edwin, P. M.: 1992, *Ann. Geophys.* (in press).
Edwin, P. M. and Roberts, B.: 1988, *Astron. Astrophys.* **192**, 343.
Harrison, R. A.: 1987, *Astron. Astrophys.* **182**, 337.
Kane, S. R., Kai, K., Kosugi, T., Enome, S., Landecker, P. B., and McKenzie, D. L.: 1983, *Astrophys. J.* **271**, 376.
Krüger, A.: 1979, *Introduction to Solar Radio Astronomy and Radio Physics*, D. Reidel Publ. Co., Dordrecht, Holland.
Kurths, J. and Karlický, M.: 1989, *Solar Phys.* **119**, 399.
Murawski, K. and Edwin, P. M.: 1992, *J. Plasma Phys.* **47**, 75.
Murawski, K. and Roberts, B.: 1993a, *Solar Phys.* **143**, 89 (Paper I).
Murawski, K. and Roberts, B.: 1993b, *Solar Phys.* **144**, 101 (Paper II).
Murawski, K. and Roberts, B.: 1993c, *Solar Phys.* **144**, 255 (Paper III).
Pasachoff, J. M.: 1990, in E. R. Priest and P. Ulmschneider (eds.), *Mechanisms of Chromosphere and Coronal Heating*, Springer-Verlag, Heidelberg, p. 25.
Qi-Jun, F., Yuan-Fang, G., Sheng-Zhen, J., and Ren-Yang, Z.: 1990, *Solar Phys.* **130**, 161.
Ren-Yang, Z., Sheng-Zhen, J., Qi-Jun, F., and Xiao-Cong, L.: 1990, *Solar Phys.* **130**, 151.
Roberts, B., Edwin, P. M., and Benz, A. O.: 1983, *Nature* **305**, 688.
Roberts, B., Edwin, P. M., and Benz, A. O.: 1984, *Astrophys. J.* **279**, 857.
Takakura, T., Kaufmann, P., Costa, J. E. R., Degaonkar, S. S., Ohki, K., and Nitta, N.: 1983, *Nature* **302**, 317.
Tapping, K. F.: 1978, *Solar Phys.* **59**, 145.